nature microbiology

SUPPLEMENTARY INFORMATION

https://doi.org/10.1038/s41564-018-0275-7

In the format provided by the authors and unedited.

Atomic structures of enterovirus D68 in complex with two monoclonal antibodies define distinct mechanisms of viral neutralization

Qingbing Zheng[1,6], Rui Zhu[1,6], Longfa Xu[1,6], Maozhou He[1,6], Xiaodong Yan[1,2,6], Dongxiao Liu[1], Zhichao Yin[1], Yangtao Wu[1], Yongchao Li[1], Lisheng Yang[1], Wangheng Hou[1], Shuxuan Li[1], Zizhen Li[1], Zhenqin Chen[1], Zhihai Li[1], Hai Yu[1], Ying Gu[1], Jun Zhang[1], Timothy S. Baker[2,7], Z. Hong Zhou[3,4,7], Barney S. Graham[5]*, Tong Cheng[1]*, Shaowei Li[1]* and Ningshao Xia[1]*

[1]State Key Laboratory of Molecular Vaccinology and Molecular Diagnostics, National Institute of Diagnostics and Vaccine Development in Infectious Diseases, School of Life Science, School of Public Health, Xiamen University, Xiamen, China. [2]Department of Chemistry and Biochemistry and Division of Biological Sciences, University of California, San Diego, San Diego, CA, USA. [3]The California NanoSystems Institute, UCLA, Los Angeles, CA, USA. [4]Department of Microbiology, Immunology and Molecular Genetics, University of California, Los Angeles, Los Angeles, CA, USA. [5]Vaccine Research Center, National Institute of Allergy and Infectious Diseases, National Institutes of Health, Bethesda, MD, USA. [6]These authors contributed equally: Qingbing Zheng, Rui Zhu, Longfa Xu, Maozhou He, Xiaodong Yan.[7]These authors jointly supervised this work: Z. Hong Zhou and Timothy S. Baker.
*e-mail: bgraham@nih.gov; tcheng@xmu.edu.cn; shaowei@xmu.edu.cn; nsxia@xmu.edu.cn

Supplementary Information

Atomic Structures of Enterovirus D68 in Complex with Two Monoclonal Antibodies Define Distinct Mechanisms of Viral Neutralization

Qingbing Zheng[1,6], Rui Zhu[1,6], Longfa Xu[1,6], Maozhou He[1,6], Xiaodong Yan[1,2,6], Dongxiao Liu[1], Zhichao Yin[1], Yangtao Wu[1], Yongchao Li[1], Lisheng Yang[1], Wangheng Hou[1], Shuxuan Li[1], Zizhen Li[1], Zhenqin Chen[1], Zhihai Li[1], Hai Yu[1], Ying Gu[1], Jun Zhang[1], Timothy S. Baker[2], Z. Hong Zhou[3,4], Barney S. Graham[5,*], Tong Cheng[1,*], Shaowei Li[1,*], Ningshao Xia[1,*]

[1]State Key Laboratory of Molecular Vaccinology and Molecular Diagnostics, National Institute of Diagnostics and Vaccine Development in Infectious Diseases, School of Life Science, School of Public Health, Xiamen University, Xiamen, 361102, PR China

[2]Department of Chemistry and Biochemistry and Division of Biological Sciences, University of California, San Diego, San Diego, CA 92093-0378, USA

[3]The California NanoSystems Institute (CNSI), UCLA, Los Angeles, California 90095, USA

[4]Department of Microbiology, Immunology and Molecular Genetics, University of California, Los Angeles, Los Angeles, CA 90095, USA

[5]Vaccine Research Center, National Institute of Allergy and Infectious Diseases, National Institutes of Health, Bethesda, MD 20892, USA

[6]These authors contributed equally to this work.

*Correspondence should be addressed to N.X. (nsxia@xmu.edu.cn), S.L. (shaowei@xmu.edu.cn), T.C. (tcheng@xmu.edu.cn), or B.S.G.(bgraham@nih.gov).

Supervising author should be addressed to Z.H.Z. (hong.zhou@ucla.edu) and T.S.B. (tsb@ucsd.edu)

Supplementary Figures

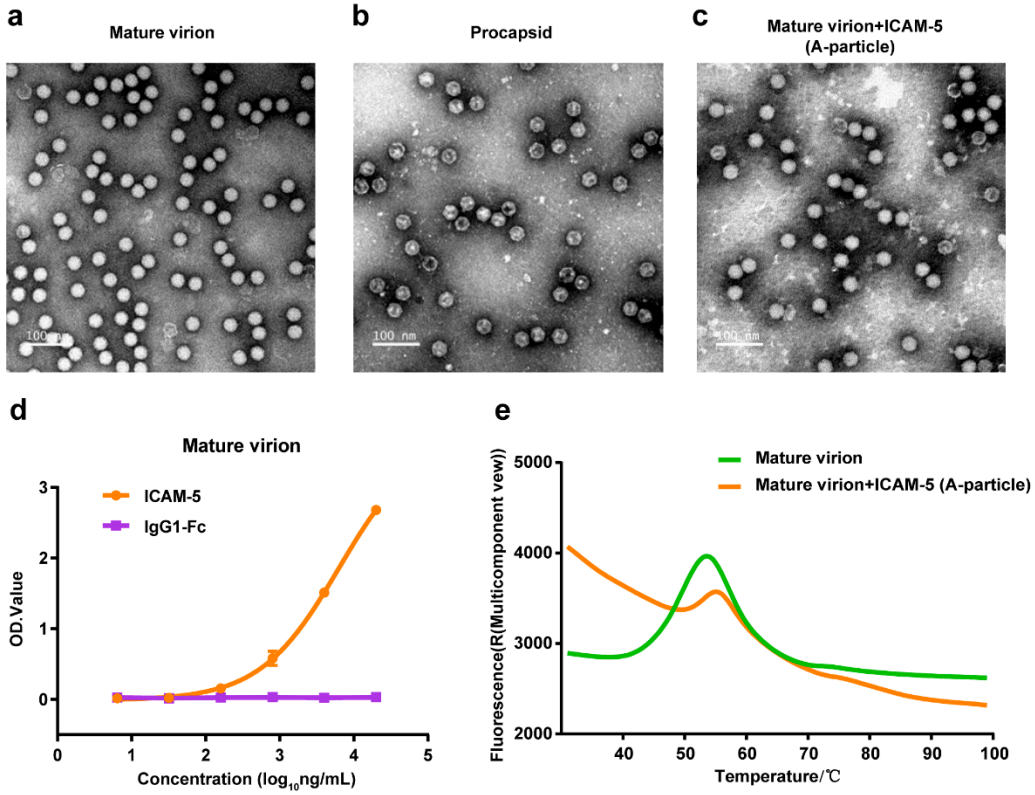

Supplementary Figure 1. Characterizations of EV-D68 particles and their complexes with cell receptor ICAM-5.

(a-c) Negative staining electron microscopy of EV-D68 mature virions **(a)**, procapsids **(b)** and A-particles **(c)**. A-particles are those induced by ICAM-5 binding of the purified mature virions. Three batches of mature virions, procapsids and ICAM-5 induced A-particles were independently prepared and respectively checked with negative staining electron microscopy. The particle morphology is consistent within each type, in which only one representative micrograph is shown.

(**d)** Analysis of the binding of ICAM-5 to EV-D68 mature virions by binding ELISA which was performed by coating with purified EV-D68 mature virions. Various concentrations of ICAM-5 or human IgG1-Fc control proteins were added in triplicate. The amount of bound ICAM-5 or control IgG1-Fc are presented as average OD450 ± SD.

(**e)** PaSTRy assay of EV-D68 mature virions and their complexes with ICAM-5 (A-particles). The fluorescence traces are shown for EV-D68 mature virions (green line) as well as their complexes with ICAM-5 (orange line). Experiments were repeated in triplicate.

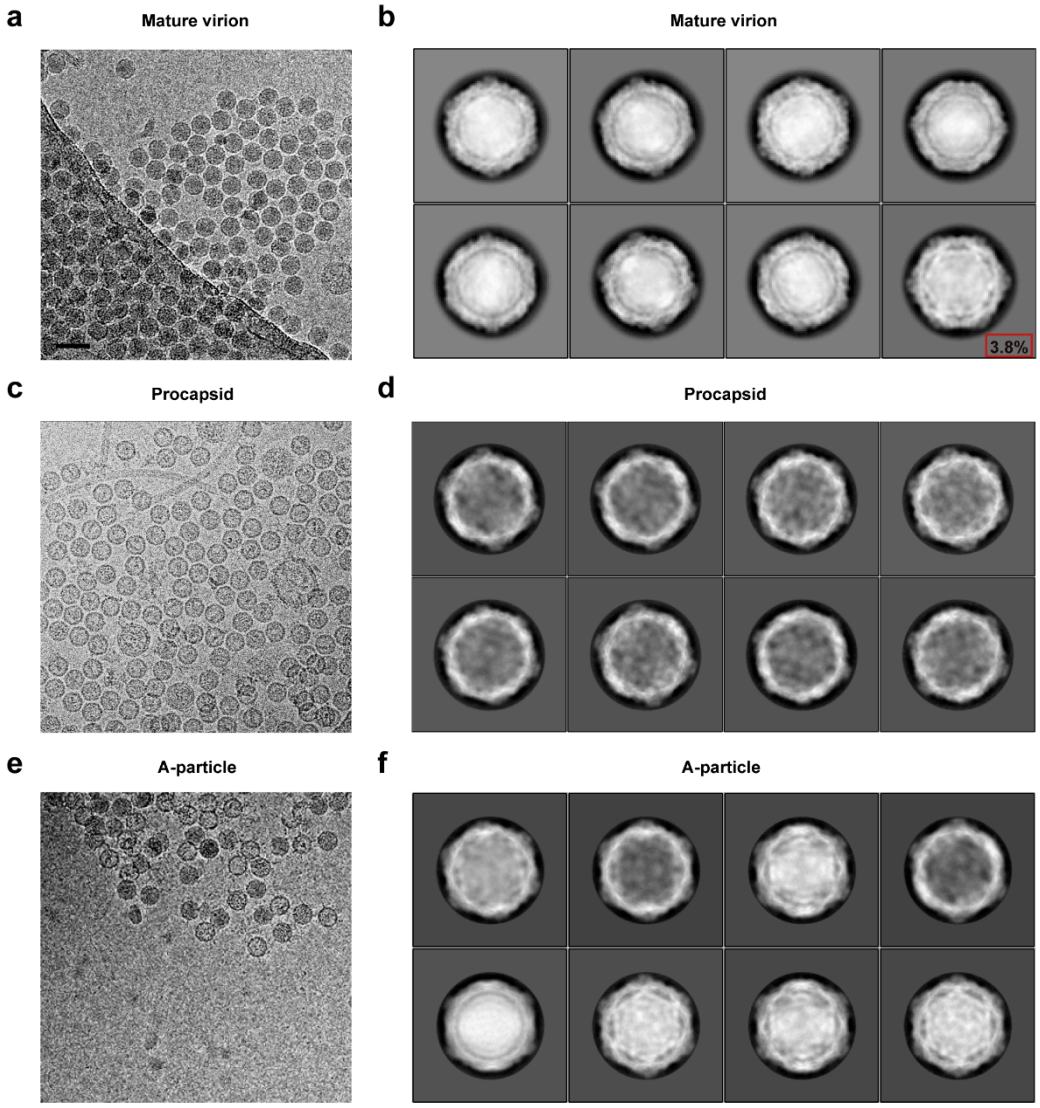

Supplementary Figure 2. CryoEM micrographs and 2D image processing of three different types of EV-D68 particles.
(a, c, e) Representative motion corrected (from 17 movie frames) micrographs of EV-D68 mature virions **(a)**, procapsids **(c)** and A-particles **(e)**. Scale bar = 50 nm.
(b, d, f) Representative 2D classification averages of above three kinds of particles. Of note, a small part of 3.8% of particles were sorted out during image 2D classification of mature virions that distinguish to the other particles which were further identified as A-particles from virus-infected cells (A-particel_us). In the sample of A-particle triggered by ICAM-5 **(e, f)**, it also contains some parts of mature virions and empty particles.

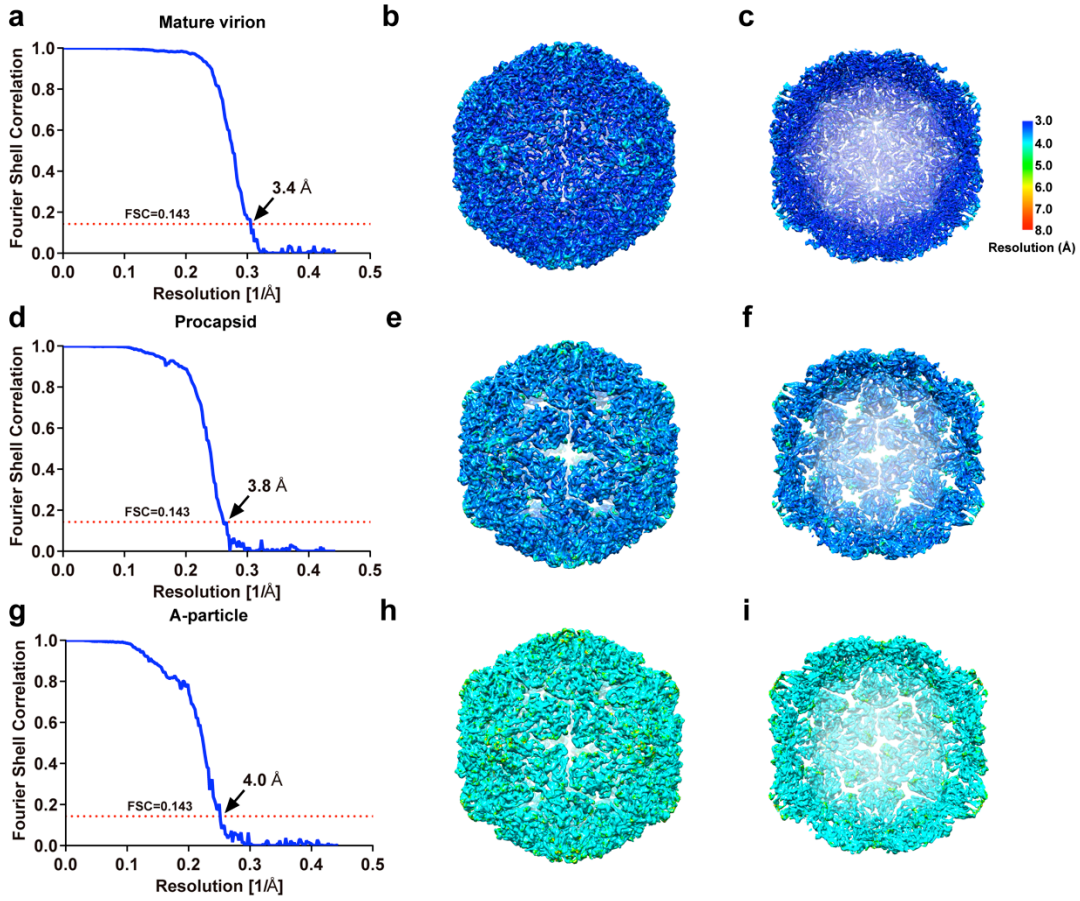

Supplementary Figure 3. Global and local resolution analysis of 3D reconstructions of EV-D68 mature virion, procapsid and A-particle.
(a, d, g) Fourier shell correlation (FSC) curves of 3D reconstructions of EV-D68 mature virion **(a)**, procapsid **(d)** and A-particle **(g)** were plotted against spatial frequency. Resmap analysis of the structures of mature virion **(b-c)**, procapsid **(e-f)** and A-particle **(g-h)**.

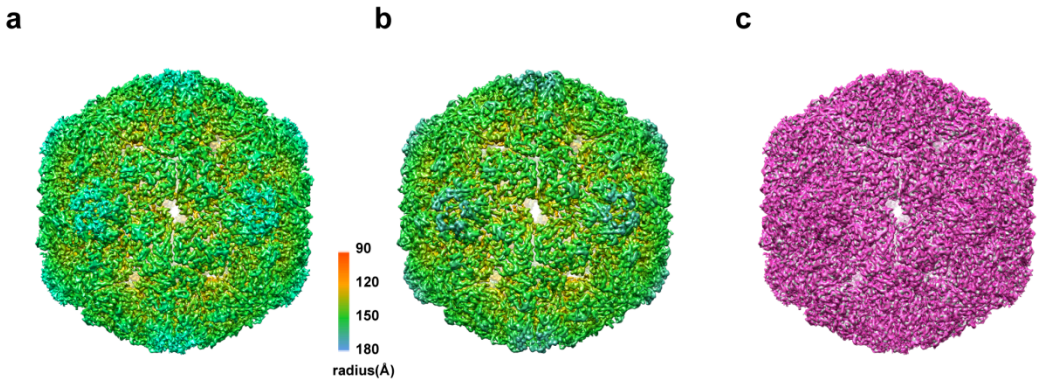

Supplementary Figure 4. The 4.4 Å cryoEM structure of A-particle_us sorted out from the sample of mature virion.
(a, b) The iso-contoured views of cryoEM maps of A-particle_us **(a)** and A-particle_i5 **(b)** (radially colored) are shown. The density map of A-particle_us was reconstructed by sorting a subset of particles distinguished during image processing of the mature virions. The density map of A-particle_i5 **(b)** was low-pass filtered to 4.4 Å. **(c)** Comparison of A-particle_us (magenta) and A-paritcle_i5 (gray) shows highly structural similarity (correlation coefficient 0.99).

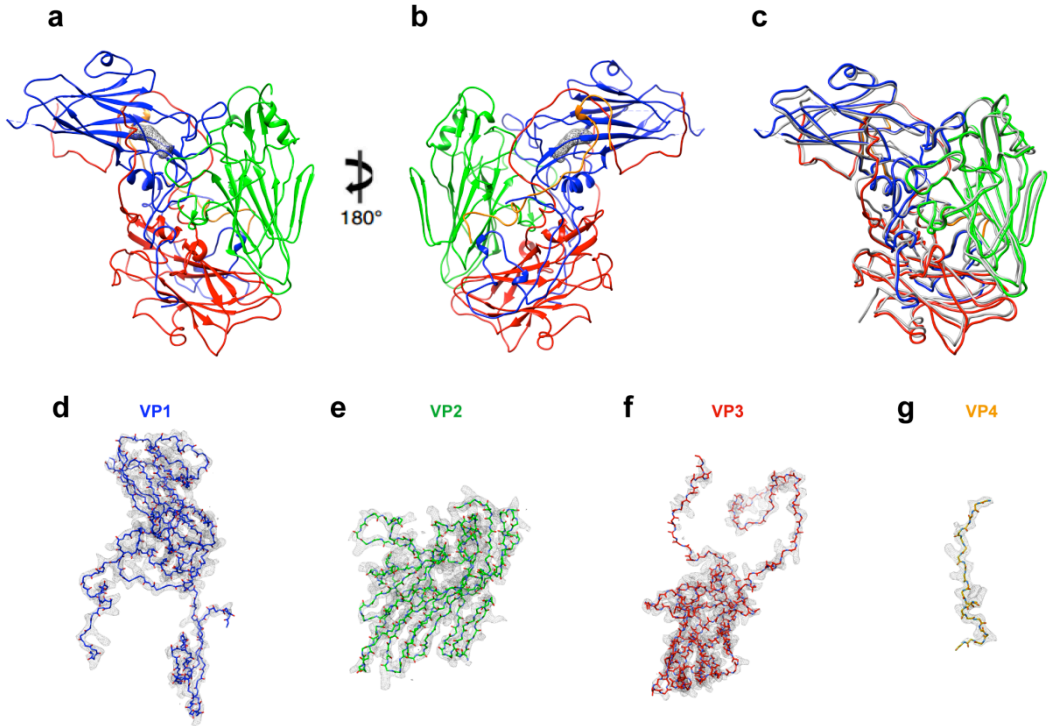

Supplementary Figure 5. Atomic model of the protomer of EV-D68 mature virion.
(a, b) The model of one protomer of EV-D68 capsid structure contains VP1 (blue), VP2 (green), VP3 (red) and VP4 (orange), the hydrophobic pocket is shown as gray mesh.
(c) Superposition of our structure and the crystal structure of EV-D68 Fermon strain (gray) (PDB code 4wm8).
(d-g) The density maps and fitted models of individual VP1 **(d)**, VP2 **(e)**, VP3 **(f)** and VP4 **(g)**.

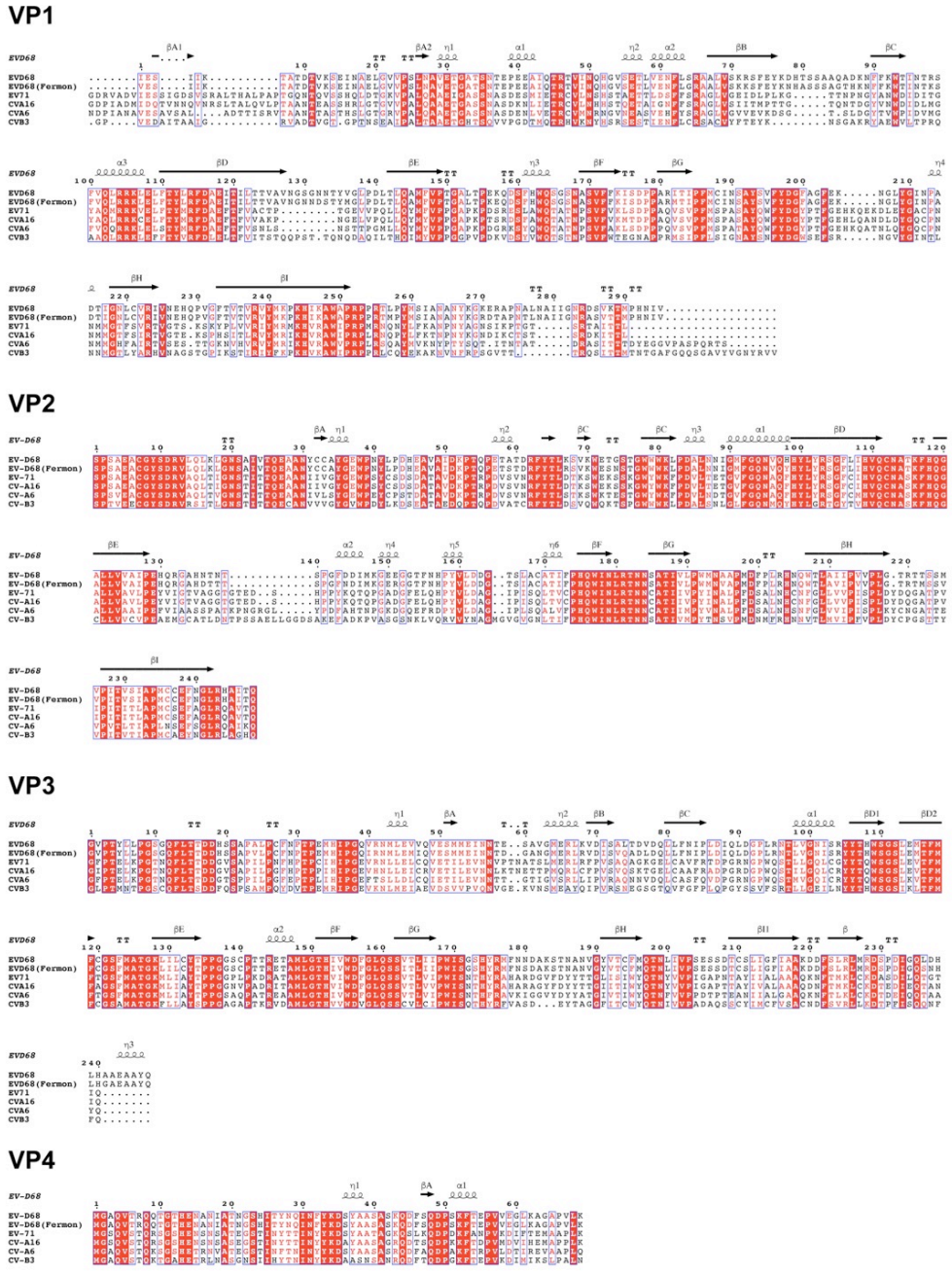

Supplementary Figure 6. Espript representation of a structure-based sequence alignment.

Espript representation of a structure-based sequence alignment of VP1, VP2, VP3 and VP4 of EV-D68 (GenBank accession no. *KM881710*) with EV-D68 Fermon strain (GenBank accession no. *AY426531.1*) and four other representative picornaviruses EV-71, CV-A16, CV-A6 and CV-B3 (GenBank accession no. *FJ600325*, *FJ198212*, *KR706309*, *M88483*, respectively). Secondary structure elements are indicated above the sequence.

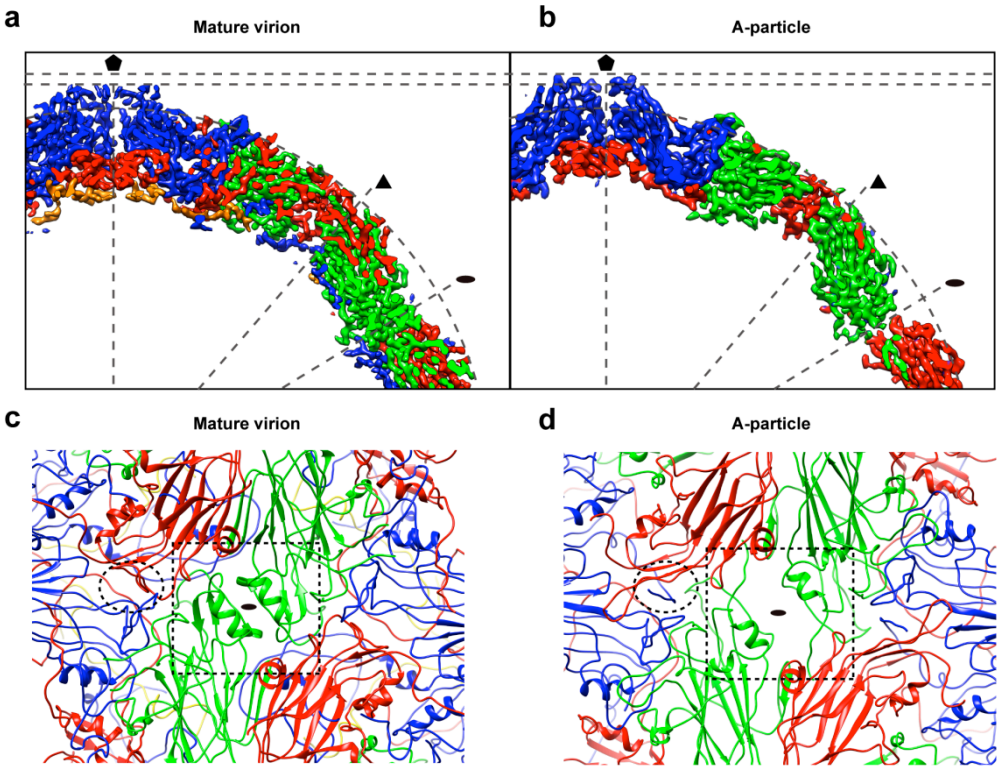

Supplementary Figure 7. Structure comparison of EV-D68 mature virion and A-particle.
(a, b) Cross sections of the density maps of EV-D68 mature virion **(a)** and A-particle **(b)** show the latter with a larger radius along 5-fold axis.
(c, d) Close up views centered at a 2-fold axis (black ellipses) of atomic models of EV-D68 mature virion **(c)** and A-particle **(d)**. The 2-fold channels (dashed squares) are wider in A-particle than mature virion. An externalized VP1 N-terminus of A-particle in **(d)** is marked by dashed ellipse.

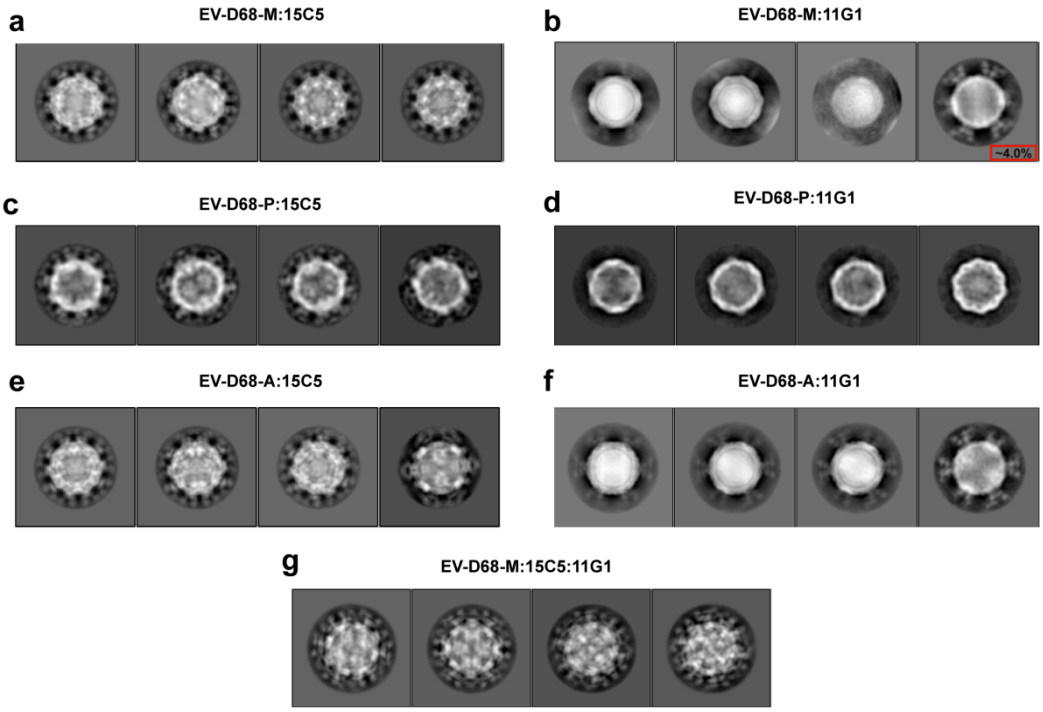

Supplementary Figure 8. 2D classification results of three types of particles in complex with NAb-Fabs.
(a-g) 2D classification results of three types of particles in complex with Fab 15C5 **(a, c, e)**, 11G1 **(b, d, f)** or both **(g)** showing different binding efficiency of two NAbs. Of note, for the sample of EV-D68-M:11G1, only the small part of A-particle_us (~4%) were efficiently occupied by Fabs.

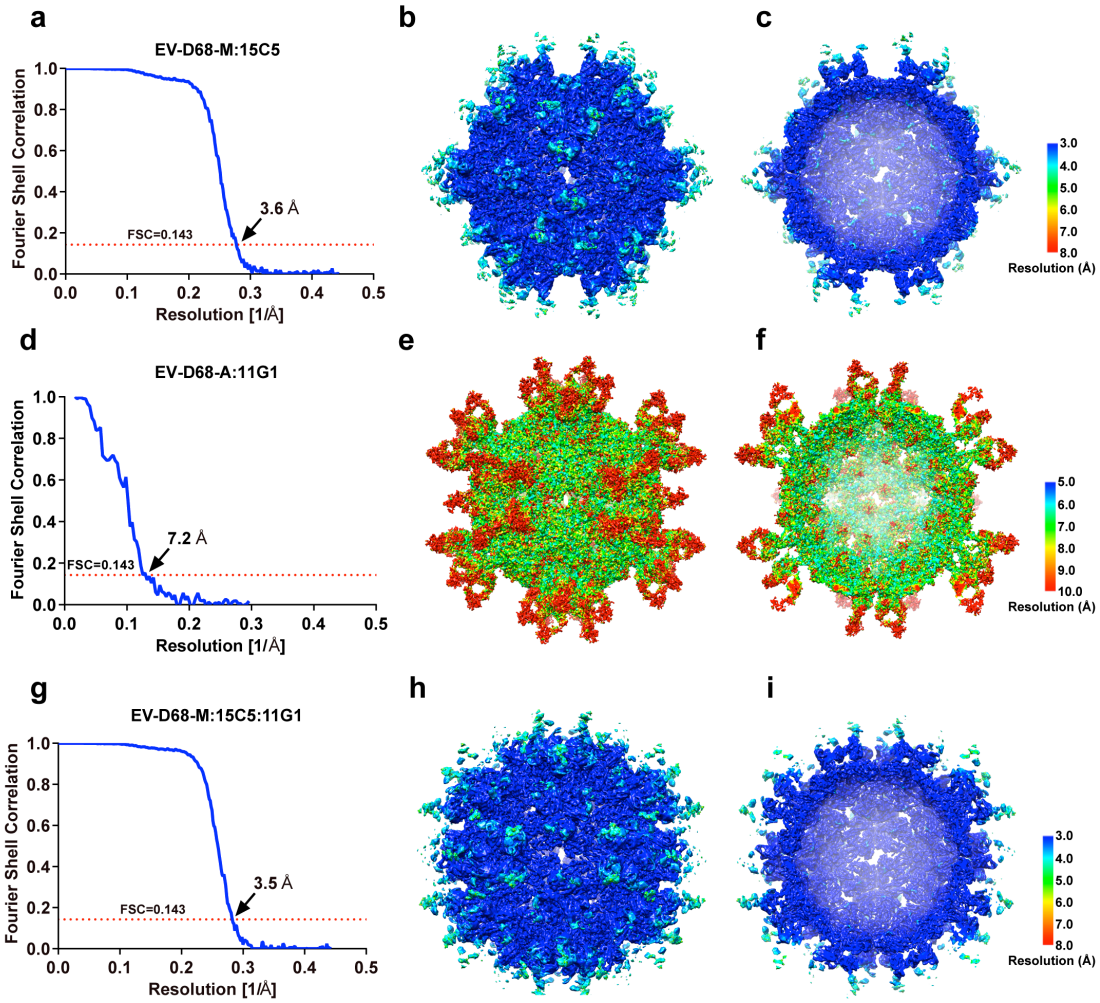

Supplementary Figure 9. Global and local resolution analysis of 3D reconstructions of EV-D68 immune-complexes.
(a, d, g) Fourier shell correlation (FSC) curves of 3D reconstructions of EV-D68-M:15C5 **(a)**, EV-D68-A:11G1 **(d)** and EV-D68-M:15C5:11G1 **(g)** were plotted against spatial frequency. Resmap analysis of the structures of EV-D68-M:15C5 **(b-c)**, EV-D68-A:11G1 **(e-f)** and EV-D68-M:15C5:11G1 **(h-i)**.

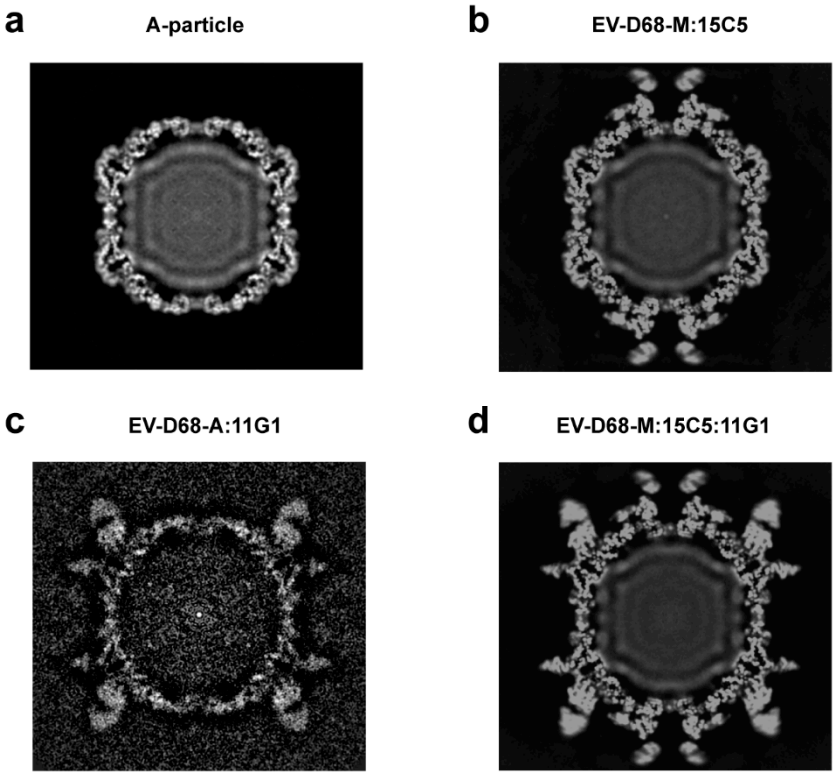

Supplementary Figure 10. Central sections of density maps.
(a-d) Central sections of density maps of EV-D68 A-particle **(a)**, EV-D68-M:15C5 **(b),** EV-D68-A:11G1 **(c)** and EV-D68-M:15C5:11G1 **(d)**. EV-D68 A-particle, EV-D68-M:15C5 and EV-D68-M:15C5:11G1 show similar genomic RNA organization.

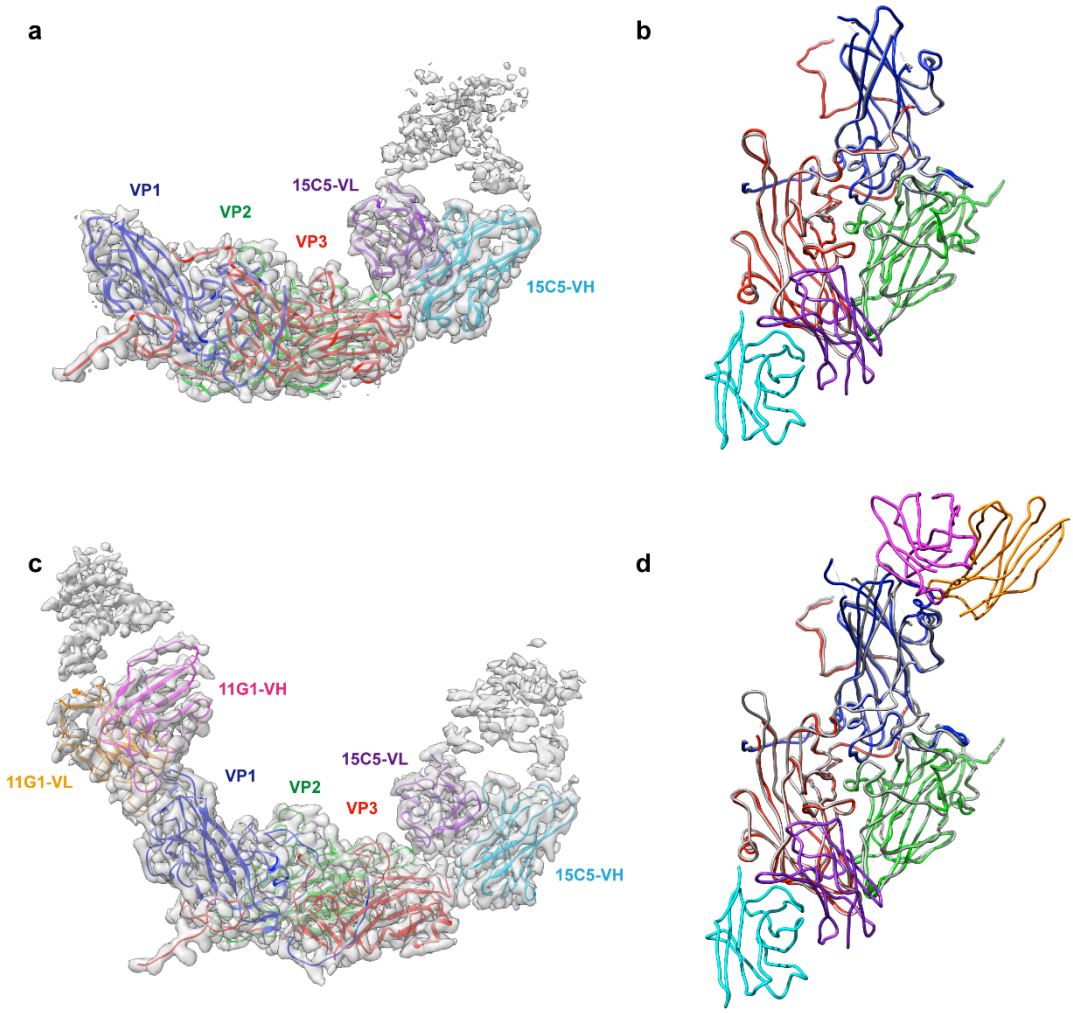

Supplementary Figure 11. The segmented asymmetric units of immune-complex density maps fitted with related models.
(a, c) The segmented asymmetric units of EV-D68-M:15C5 **(a)** and EV-D68-M:15C5:11G1 **(c)** immune-complex density maps (gray) fitted with related models (ribbon diagrams). The models of 15C5 heavy chain (15C5-VH), 15C5 light chain (15C5-VL), 11G1 heavy chain (11G1-VH) and 11G1 light chain (11G1-VL) were colored in cyan, purple, magenta and orange respectively. The Fab constant domains of two immune-complexes exhibits weak densities at the contour level of 3σ.
(b, d) Superpositions of protomers of A-particle (gray) with that of EV-D68-M:15C5 **(b)** or EV-D68-M:15C5:11G1 **(d)**. Models of complexes are colored as the same in **(a)** and **(c)**.

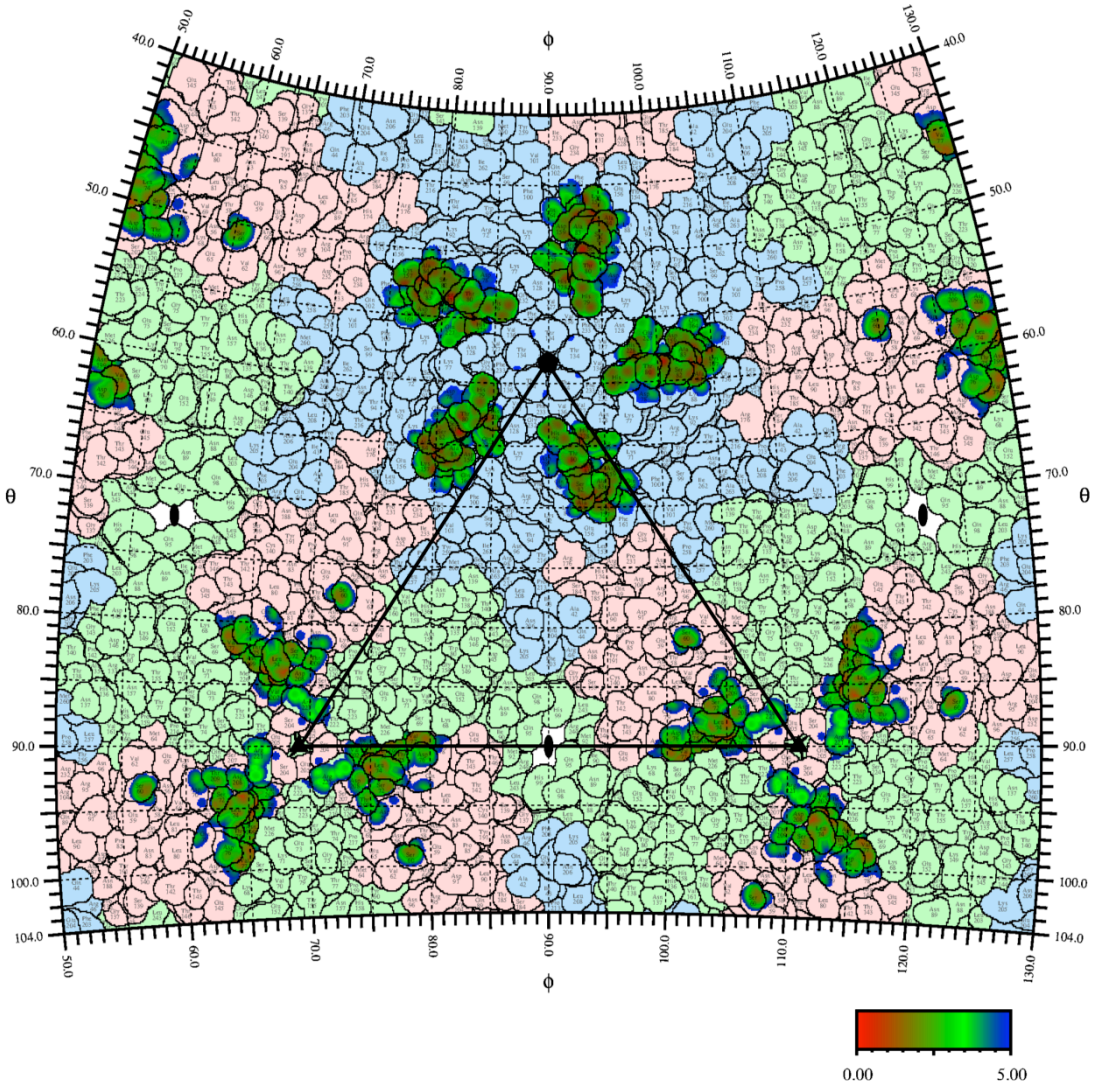

Supplementary Figure 12. The footprints of Fab-15C5 and Fab-11G1 on EV-D68 capsid.

Residues of VP1, VP2 and VP3 are outlined in light blue, light green and light red, respectively. The footprints of Fab-15C5 (around 3-fold) and Fab-11G1 (around 5-fold) are highlighted and colored according to the atomic distance of particle surface to Fab from red to blue. The black triangle shows an icosahedral asymmetric unit of the EV-D68 structure. Figure was prepared with software RIVEM.

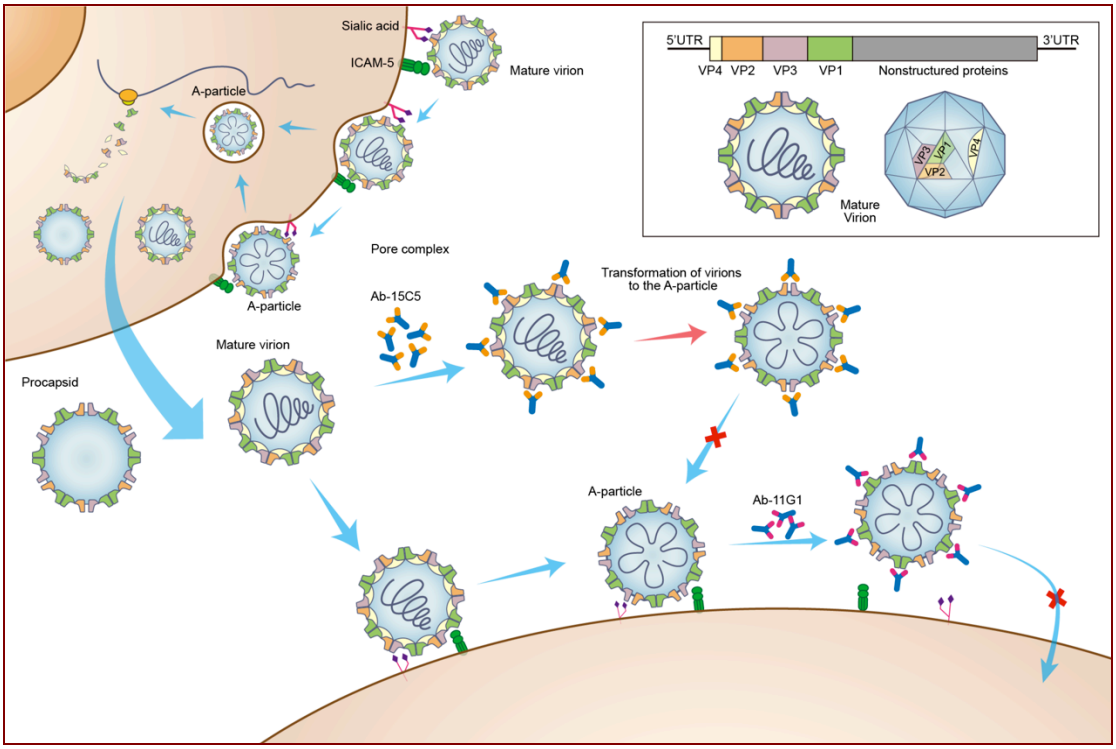

Supplementary Figure 13. Proposed schematic model for EV-D68 life cycle and stages neutralized by 15C5 and 11G1.

Upon binding cellular receptors such as sialic acid or ICAM-5, EV-D68 mature virions transform into A-particles within endosomes or on the host cell surface prior to endocytosis. A-particles then undergo uncoating and release genomic RNA into cytosol. Progeny mature virions and procapsids without genomes are released from infected cell. NAb 15C5 can bind all three forms of particles. It can trigger the transformation of mature virions to A-particles and neutralize virus pre-attachment. In contrast, NAb 11G1 exclusively recognizes A-particles, and it appears to recognize viruses only after their attaching to cell surface receptors and subsequently undergoing transformation to A-particles. Therefore, NAb 11G1 may neutralize virus via a post-attachment manner.

Supplementary Tables

Supplementary Table 1. Statistics of 3D reconstructions and model refinement.

	Mature virion(EV-D68-M) (EMDB-9629) (PDB 6AJ0)	Procapsid (EV-D68-P) (EMDB-9632) (PDB 6AJ3)	A-particle_i5 (EMDB-9631) (PDB 6AJ2)	A-particle_us (EMDB-9635)	EV-D68-M:15C5 (EMDB-9633) (PDB 6AJ7)	EV-D68-M:15C5:11G1 (EMDB-9634) (PDB 6AJ9)	EV-D68-A:11G1 (EMDB-9636)
Data collection and processing							
Magnification	x93,000	x93,000	x93,000	x93,000	x93,000	x93,000	x93,000
Voltage (kV)	300	300	300	300	300	300	300
Electron exposure (e–/Å^2)	25	25	25	25	25	25	25
Defocus range (μm)	-0.7 to -2.8	-0.9 to -3.6	-0.8 to -3.8	-0.7 to -2.8	-0.7 to -4.1	-1.0 to -4.5	-1.7 to -4.2
Pixel size (Å)	1.128	1.128	1.128	1.128	1.128	1.128	1.128
Symmetry imposed	I2	I2	I2	I2	I2	I2	I2
Initial particle images (no.)	45,822	14,265	25,045	45,822	105,346	143,304	414
Final particle images (no.)	11,938	13,849	9,625	2,491	58,540	102,512	375
Map resolution (Å)	3.4	3.8	4.0	4.4	3.6	3.5	7.2
FSC threshold	0.143	0.143	0.143	0.143	0.143	0.143	0.143
Map resolution range (Å)	3.0-8.0	3.0-8.0	3.0-8.0	n/a	3.0-8.0	3.0-8.0	5.0-10.0
Refinement							
Initial model used (PDB code)	4wm8	5xs4	5xs4	n/a	5xs7	5xs7	n/a
Model resolution (Å)	3.5	4.1	4.2	n/a	3.6	3.6	n/a
FSC threshold	0.5	0.5	0.5		0.5	0.5	
Model resolution range (Å)	3.5	4.1	4.2		3.6	3.6	
Map sharpening *B* factor (Å^2)	-206.37	-238.06	-222.19	-252.26	-230.01	-237.26	n/a
Model composition				n/a			n/a
Non-hydrogen atoms	6,163	4,487	5,355		7,055	8,694	
Protein residues	789	573	682		901	1,112	
Ligands	1	0	0		0	0	
B factors (Å^2)	n/a	n/a	n/a	n/a	n/a	n/a	n/a
Protein							
Ligand							
R.m.s. deviations				n/a			n/a
Bond lengths (Å)	0.0095	0.0081	0.0052		0.0083	0.0073	
Bond angles (°)	1.25	1.23	1.21		1.3	1.25	
Validation				n/a			n/a
MolProbity score	1.46	1.60	1.60		1.68	1.57	
Clashscore	3.03	4.83	3.12		4.03	2.8	
Poor rotamers (%)	0.00	0.00	0.00		0.00	0.00	
Ramachandran plot				n/a			n/a
Favored (%)	94.98	94.97	91.82		91.86	92.21	
Allowed (%)	4.89	5.03	8.18		8.14	7.79	
Disallowed (%)	0.13	0.00	0.00		0.00	0.00	

Supplementary Table 2. Structural comparison (RMSD) of capsid proteins of EV-D68 in different particle forms.

Particle forms	RMSD	VP1	VP2	VP3	VP4	Total
protomer of mature VS Fermon (crystal structure)	a.a. number	271	235	247	32	**785**
	RMSD	0.97	1.03	1.20	1.20	**1.07**
protomer of A-particle VS procapsid	a.a. number	186	166	220	/	**572**
	RMSD	0.93	0.61	0.64	/	**0.73**
protomer of A-particle VS 15C5 complex	a.a. number	204	232	246	/	**682**
	RMSD	0.60	0.44	0.44	/	**0.49**
protomer of A-particle VS triple immune-complex	a.a. number	204	232	227	/	**663**
	RMSD	1.07	0.56	0.85	/	**0.82**

Supplementary Table 3. Interaction contacts of 15C5 revealed by immune-complexes.

EV-D68-M:15C5 interaction residues					
domains		residues	distance (Å)	Fab-15C5	CDR
VP3	AB loop	S60 [OG]	3.29	S60 [OG]	LFR2
	BC loop	S72 [OG]	3.29	Y49 [OH]	LCDR2
		L74 [CD1]	3.34	S106 [OG]	HCDR3
		L74 [CD2]	3.40	Y104 [CG]	HCDR3
		L74 [CD2]	3.30	Y104 [CD2]	HCDR3
		D76 [OD1]	3.15	Y32 [OH]	HCDR1
		D76 [OD1]	3.30	Y32 [CE1]	HCDR1
		D76 [OD1]	3.83	R98 [NH1]	HCDR3
	HI loop	N199 [ND2]	3.42	G102 [N]	HCDR3
		D208 [OD2]	3.79	S50 [OG]	LCDR2
VP2*	BC loop	K67 [NZ]	3.83	T28 [OG1]	HCDR1
		K70 [NZ]	2.55	N31 [O]	HCDR1
		K70 [NZ]	2.85	F101 [O]	HCDR3
		K70 [NZ]	2.98	N103 [ND2]	HCDR3
		K70 [CE]	3.11	F101 [O]	HCDR3
		E72 [OE1]	2.61	N52 [ND2]	HCDR2
		S75 [OG]	3.86	N54 [ND2]	HCDR2
	HI loop	S224 [O]	3.44	N103 [CG]	HCDR3
		S224 [O]	2.41	N103 [OD1]	HCDR3
		S224 [CB]	3.48	N103 [OD1]	HCDR3
		M225 [SD]	3.36	G102 [CA]	HCDR3

The interaction residues were computed using the PISA server (http://www.ebi.ac.uk/msd-srv/prot_int/pistart.html). Hydrogen-bond distances cut-off: 4.0 Å; salt-bridge distance cut-off: 4.0 Å. The red fonts refer to hydrogen bonds and the green background refers to salt-bridge.

* refers to viral domains from adjacent protomer.

Supplementary Table 4. Interaction contacts of 11G1 revealed by immune-complexes.

EV-D68-M:11G1 interaction residues					
domains		residues	distance (Å)	Fab-11G1	CDR
VP1	BC loop	T80 [CA]	3.48	G104 [O]	HCDR3
		T80 [OG1]	3.82	G104 [O]	HCDR3
		T80 [OG1]	3.08	S106 [OG]	HCDR3
		S81 [N]	2.88	G104 [O]	HCDR3
		S81 [OG]	3.49	G104 [O]	HCDR3
		S81 [O]	3.47	G104 [O]	HCDR3
		S81 [O]	3.45	S106 [CB]	HCDR3
		S81 [O]	3.15	S106 [N]	HCDR3
		S81 [O]	2.54	S106 [OG]	HCDR3
		S81 [C]	3.33	S106 [OG]	HCDR3
		S82 [OG]	2.78	Y98 [O]	LCDR3
		S82 [OG]	3.58	Y100 [N]	LCDR3
		S82 [OG]	3.32	N99 [CA]	LCDR3
		A83 [O]	3.18	Y31 [CD1]	LCDR1
		A83 [O]	3.22	Y31 [CE1]	LCDR1
		A83 [O]	3.35	Y98 [CE1]	LCDR3
		A83 [N]	3.37	Y98 [O]	LCDR3
		A83 [C]	3.40	Y98 [O]	LCDR3
		A84 [CB]	3.49	Y98 [O]	LCDR3
		A84 [N]	3.05	Y98 [O]	LCDR3
		D87 [OD1]	3.41	S32 [CB]	LCDR1
		D87 [OD1]	3.21	S32 [OG]	LCDR1
		D87 [OD2]	3.00	S32 [OG]	LCDR1
		D87 [OD2]	3.39	S32 [N]	LCDR1
		D87 [OD2]	2.97	Y98 [OH]	LCDR3
	EF loop	K157 [NZ]	3.25	L30 [O]	LCDR1
		K157 [CD]	3.23	S32OG]	LCDR1
		D159 [O]	2.75	S32 [CB]	LCDR1
			3.30	S32 [OG]	LCDR1
	HI loop	H228 [O]	3.22	Y103 [O]	HCDR3
		Q229 [CB]	3.39	Y103 [O]	HCDR3
VP1*	β strand	E75 [OE1]	3.46	Y103 [OH]	HCDR3
		K77 [NZ]	3.35	Y102 [CD1]	HCDR3
	DE loop	V127 [O]	3.49	Y103 [CD1]	HCDR3
		N128 [CB]	3.50	Y102 [O]	HCDR3
		N128 [CG]	3.36	Y102 [O]	HCDR3
		N128 [ND2]	3.26	Y102 [O]	HCDR3
	β strand	T234 [OG1]	3.7	Y103 [OH]	HCDR3

The interaction residues were computed using the PISA server (http://www.ebi.ac.uk/msd-srv/prot_int/pistart.html). Hydrogen-bond distance cut-off: 4.0 Å; The red fonts refer to hydrogen bonds.

* refers to viral domains from adjacent protomer.

Supplementary Video 1

Conformational changes of a protomer when EV-D68 mature virion transforms (triggered by ICAM-5) into A-particle. The protomer rotates counterclockwise by about 3.5° with the pivot point located at the corner of VP3. The pocket-factor binding region is collapsed, the VP1 N-terminal is externalized and the VP4 is lost during such transition.